Dissociative electron attachment resonances in ammonia: A velocity slice imaging based study

N. Bhargava Ram and E. Krishnakumar

Citation: J. Chem. Phys. **136**, 164308 (2012); doi: 10.1063/1.4705358
View online: http://dx.doi.org/10.1063/1.4705358
View Table of Contents: http://jcp.aip.org/resource/1/JCPSA6/v136/i16
Published by the American Institute of Physics.

Dissociative electron attachment resonances in ammonia: A velocity slice imaging based study

N. Bhargava Ram[1,a)] and E. Krishnakumar[2,b)]
[1]*LaserLab and Physical Chemistry, Vrije Universiteit, Amsterdam 1081 HV, The Netherlands*
[2]*Tata Institute of Fundamental Research, Mumbai 400005, India*

(Received 19 November 2011; accepted 6 April 2012; published online 26 April 2012)

Negative ion resonance states of ammonia are accessed upon capture of electrons with energy 5.5 eV and 10.5 eV, respectively. These resonance states dissociate to produce H^- and NH_2^- fragment anions via different fragmentation channels. Using the velocity slice imaging technique, we measured the angular and kinetic energy distribution of the fragment H^- and NH_2^- anions with full 0–2π angular coverage across the two resonances. The scattered H^- ions at both resonances show variation in their angular distribution as a function of the kinetic energy indicating geometric rearrangement of NH_3^{-*} ion due to internal excitations and differ from the equilibrium geometry of the neutral molecule. The second resonance at 10.5 eV shows strong forward-backward asymmetry in the scattering of H^- and NH_2^- fragment ions. Based on the angular distributions of the H^- ions, the symmetry of the resonances at 5.5 eV and 10 .5 eV are determined to be A_1 and E, respectively, within C_{3v} geometry.
 [http://dx.doi.org/10.1063/1.4705358]

I. INTRODUCTION

Electron mediated chemistry is dominant in many environments, from low density interstellar medium to complex and dense biological cells and tissues. One of the dominant processes in the interaction of low energy electrons with neutral molecules is the formation of negative ions in excited states and is often characterized by high cross sections. These negative ions states are usually repulsive, dissociating into an anion fragment, and neutrals. The fragments have high reactivity and could result in further chemistry. We have undertaken a systematic study of these negative ion resonances in small polyatomic systems in terms of their cross sections, fragment energy, and angular distributions to characterize and understand the dissociation dynamics therein.

Studies on electron induced chemistry in ammonia are very important for many reasons. Ammonia is known to play a major role in the synthesis of bigger organic molecules in the interstellar medium, amino acids. The formation of amino acids by the irradiation of ultraviolet light and high energy electron beams on mixtures of ice containing ammonia and other small molecules has been demonstrated experimentally.[1–3] Ammonia is a constituent of the atmospheres of many planets and comets. The measurements on ammonia also assume importance in the context of engineering applications such as plasma reactors for waste treatment or plasma surface treatment.

Electron attachment studies on ammonia also assume significance in the context of the recently discovered functional group dependence in electron attachment and its relevance to chemical control using low energy electrons through site selective fragmentation.[4] It was shown that selective fragmentation of O–H, N–H, and C–H bonds in molecules are possible using electron energy as a control parameter.[4,5] In this context, it is important to study the dynamics of the process starting from the precursor molecules of the functional groups, viz., water, ammonia, methane, etc. and compare the dynamics with those in bigger molecules where the functional groups are present.

NH_3 has a pyramidal equilibrium geometry in ground state with electronic configuration $1a_1^2 2a_1^2 1e^4 3a_1^2$ leading to $^1A_1$ in C_{3v} geometry. The HOMO orbital $3a_1$ has a lobe pointing away from the three hydrogens and corresponds to the lone pair orbital localized upon the N atom, whereas the HOMO-1 orbital with 1*e* symmetry (doubly degenerate) has lobes encompassing the N and H atoms. Earlier experiments[6–9] showed ammonia to have dissociative electron attachment (DEA) peaks at 5.5 eV and 10.5 eV. The excitation of the HOMO and HOMO-1 orbitals and subsequent electron attachment to these valence excited states cause the negative ion resonances. Table I lists the various dissociation channels possible with their thermodynamic thresholds, corresponding anion resonance symmetries based on Wigner-Witmer correlation rules and references used to estimate the thermodynamic thresholds. Based on energetics and correlations with vacuum ultraviolet (VUV) absorption spectrum and electron energy loss experiment data, there have been speculations on the possible symmetry states accessed and the dissociation mechanisms.[6]

In two of the earliest works on DEA to ammonia, Sharp and Dowell[6] and Compton *et al.*[7] measured the cross sections for total negative ion yield and fragment anions (H^- and NH_2^- mostly; NH^- is also reported) as a function of energy and isotope effects in NH_3 and ND_3 across the two resonance processes. The absolute cross sections reported by Sharp and Dowell[6] and Compton *et al.*[7] differed by about a factor of two. This uncertainty was resolved recently by Rawat *et al.*[10]

a)Electronic mail: nbhargavram@gmail.com.
b)Electronic mail: ekkumar@tifr.res.in.

TABLE I. Various dissociation channels, their appearance energies and corresponding symmetries of NH_3^{-*} within C_{3v} point group based on Wigner-Witmer correlation rules.

Dissociation channel	Thermodynamic threshold	Symmetry
$H^- + NH_2(^2B_1)$	3.85 eV (Refs. 12 and 13)	A_1
$H^- + NH_2^*(^2A_1)$	5.23 eV (Refs. 12–14)	A_1 or E
$H + NH_2^-(^1A_1)$	3.83 eV (Refs. 12 and 15)	A_1 or E
$H + NH_2^{-*}(^1A_1)$	5.98 - EA(NH_2^*) eV[a] (Refs. 12 and 14)	A_1 or E
$H^- + H + NH(^2\Sigma^-)$	7.71 eV (Refs. 12, 13, and 16)	A_2
$H + H + NH^-(^2\Pi)$	8.08 eV (Refs. 12, 16, and 17)	E

[a]Electron affinity of NH_2 in first excited state not known.

who used the pulsed electron beam and pulsed ion extraction technique along with a segmented time of flight mass spectrometer. The H^- and NH_2^- ion cross sections were found to be 2.3×10^{-18} cm^2 and 1.6×10^{-18} cm^2 at 5.5 eV and 0.5×10^{-18} cm^2 and 0.09×10^{-18} cm^2 at 10.5 eV, respectively. A comprehensive study of the DEA process at the first resonance (5.5 eV) was done by Stricklett and Burrow[8] concluding that the NH_3^{-*} resonance state decays to produce fragment ions via a predissociation mechanism similar to that in neutral excited state of ammonia.[11] They also confirmed that the negative ion undergoes umbrella mode (nv_2) oscillations as in the neutral and cation counterparts. Using symmetry arguments, they suggested that the planar dissociation of the temporary anion at 5.5 eV produces H^- whereas non planar dissociation gives rise to NH_2^-. Tronc *et al.*[9] measured the differential cross section and kinetic energy distributions of H^- and NH_2^- fragments using a 127° electrostatic energy filter and a quadrupole mass filter and found agreement with the results of Stricklett and Burrow.[8] They also measured the angular distribution of H^- ions (with kinetic energy above 1.3 eV) for incident electron energy of 5.7 eV and showed that H^- ions scatter perpendicular to the ground state dipole direction (or C_3 axis). This measurement by Tronc *et al.*[9] is the only reported measurement of angular distribution from NH_3 so far. Further, there are no measurements reported from the second resonance at 10.5 eV. It is very necessary to measure the angular distribution of the fragments as they hold direct signatures of the symmetry of the resonance states and the dissociation dynamics therein. In this paper, we present the angular and energy resolved distributions of the H^- and NH_2^- fragments across the two resonances using the velocity slice imaging technique.

II. EXPERIMENTAL SETUP

The experimental setup used has been described in detail in an earlier paper.[18] Briefly, the setup consists of a magnetically collimated and pulsed electron beam and an effusive gas beam intersecting perpendicularly. The fragment ions produced are extracted along the direction of the effusive beam towards a position sensitive detector with appropriate electrostatic focusing using a time of flight spectrometer. The pulsed extraction field is produced by applying a negative pulse across the interaction region defined by the "pusher" and "puller" electrodes and follows the electron beam after a certain time delay. The focusing conditions ensure that all ions in the entire 4π scattering sphere are collected and given mass species with given velocity are imaged onto the same point on the detector irrespective of their point of origin in a finite interaction region. The position of the hit and the time of arrival are noted for all ions. We slice the central portion (50 ns time interval) of the velocity sphere for a given mass species and retrieve the velocity slice image. By virtue of cylindrical symmetry (or azimuthal symmetry), this slice when rotated by 2π about the electron beam direction, is equivalent to the full velocity sphere. To obtain the kinetic energy distribution, the radial size of the image is calibrated using the data of O^- ions from DEA to O_2 across the 6.5 eV resonance, where the O^- ions come with a certain kinetic energy. The angular distribution is obtained by integrating ion counts over a range of the radius and in the angular range $\theta \pm 5°$ covering scattering angles from 0° to 360°. For further analysis and fitting procedures, we plot the average of the angular ranges (0°–180° and 180°–360°) i.e., average of angles symmetric about the electron beam direction to bring them to the range 0°–180°. The angular distribution plots are normalized to the intensity at 90°.

The voltages are higher for imaging light and fast moving H^- ions compared to the heavier and slower NH_2^-. The higher voltages from the focusing lens and the flight tube cause field penetration into the interaction region. This is overcome by placing a wire mesh on the aperture of the puller electrode. The imaging of the ions takes place in the presence of a magnetic field of about 40 Gauss. This results in the bending of the ion trajectories when extracted towards the detector and especially is problematic when imaging light and fast moving ions like H^-. Using an extraction field of 60 V/cm, we could image H^- ions up to 5 eV under these conditions. Since the kinetic energies of NH_2^- ions are typically a few tenths of an eV, we used a lower extraction field of 35 V/cm for imaging them. The electron energy spread in these measurements is about 0.5 eV. The contribution from this energy spread would be more in the energy distribution of the lighter fragments, while that from the Doppler spread[19] due to the target temperature would be seen more in heavier fragments. It may be noted that the earlier measurements by Tronc *et al.*[9] were confined to the angular range 20°–120° and in one plane. Whereas the present experiment collects ions scattered in the entire 4π solid angle and projects them onto a position sensitive detector thus giving scattering information over all the angles, especially forward (0°) and backward (180°) angles.

III. RESULTS AND DISCUSSION

The ion yield curve of H^- and NH_2^- produced from DEA to NH_3 (Figure 1) shows two resonance structures peaking at 5.5 eV and 10.5 eV. The curves were obtained by selecting the particular masses (mass 1 and 16, respectively) in a pure time of flight mass spectrometer mode with the detector and associated electronics in the ion counting mode and scanning the electron energy. These curves show the relative intensities of the two ions with respect to each other and are given for identifying the positions of the resonances (peaks at 5.5 and 10.5 eV) in the ion yield. A detailed discussion on the

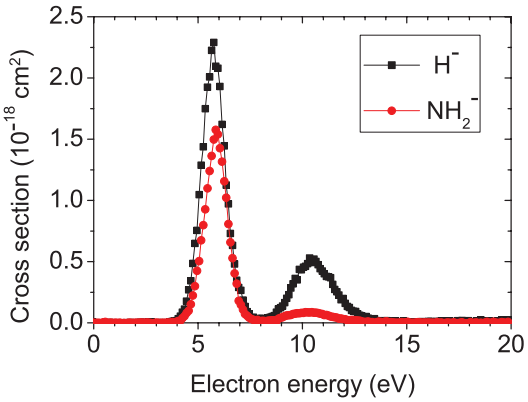

FIG. 1. DEA cross sections for H^- and NH_2^- from ammonia (adapted from Ref. 10).

absolute cross section measurement for these fragment ions is presented by Rawat *et al.*[10] Our spectrometer cannot separate NH^- and NH_2^- masses. The velocity images of H^- and NH_2^- at the two resonances are shown in Figures 2 and 6, respectively. The angular and kinetic energy distributions are discussed in Secs. III A and III B. In the process of determining both – the kinetic energy and angular distributions – we make use of only the central slice of the velocity sphere of fragment ions and do not integrate over the entire azimuthal range. The inherent cylindrical symmetry about the incident electron beam direction ensures that the distributions obtained from the central slice are similar to that obtained from the full newton sphere.

A. First resonance process peaking at 5.5 eV

The velocity slice images of H^- and NH_2^- were obtained at the resonance peak of 5.5 eV and at 1 eV away on either side of the peak. The image of H^- at 5.5 eV is shown in Figure 2(a). (Please refer to the supplementary material[24] for images at other energies). The electron beam direction is from top to bottom in every image. The H^- ions are mostly scattered perpendicular to the electron beam direction with finite intensity in other directions, including the forward (near 0°) and backward (near 180°) angles. Figure 3(a) shows the kinetic energy distribution of the H^- ions across the first resonance peak at

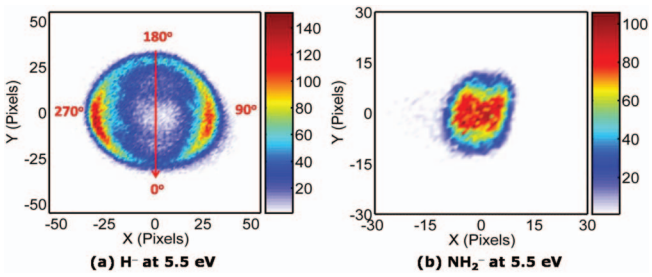

FIG. 2. Velocity slice images of H^- and NH_2^- ions from the first resonance process at 5.5 eV. The electron beam direction is from top to bottom in every image and the scattering angles are depicted with respect to the electron beam direction as shown in (a) and hold for other images similarly. The images show the impact coordinates of ions where every impact point corresponds to a particular velocity.

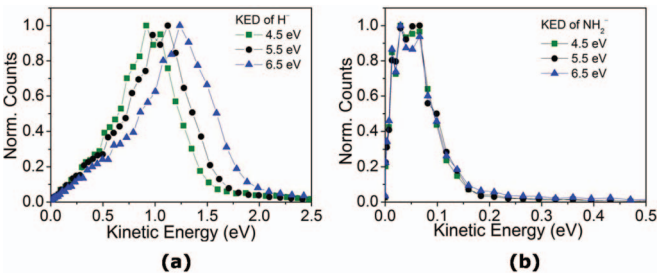

FIG. 3. Kinetic energy distribution of (a) H^- and (b) NH_2^- ions across the first resonance at 4.5, 5.5, and 6.5 eV.

electron energies 4.5, 5.5, and 6.5 eV. At the peak of the resonance, i.e., 5.5 eV, the KE ranges from 0 to about 1.8 eV and points to $H^-(^1S) + NH_2(^2B_1)$ channel with threshold at 3.85 eV. To elaborate, about 4.60 eV (Ref. 12) is needed to break the H-NH_2 bond and the electron affinity of H atom is 0.75 eV.[13] Hence, when the incident electron energy is 5.5 eV, the excess energy is about 1.65 eV and the maximum kinetic energy of H^- is estimated to be 16/17th of 1.65 eV, i.e., 1.55 eV. Given that the energy spread of H^- ions is about 0.5 eV in our experiment, the estimated value of 1.55 eV is close to the observed value of 1.8 eV. The broad kinetic energy distribution indicates internal excitation (vibrational and rotational) of the NH_2 fragment. Owing to the poorer energy resolution (~0.5 eV) of the electron beam, we are unable to see distinct rings in the velocity map image of H^- corresponding to the vibrational excitation of the NH_2 fragment. Possible presence of the $H^- + NH_2^*(^2A_1)$ channel with threshold of 5.23 eV is checked and ruled out as the kinetic energy of H^- ions in that case would be about 0.25 eV and we do not see any specific H^- ion group/lump appearing in the center of the velocity image corresponding to 0.25 eV. From Figure 3(a), we see that with increase in electron energy, the maximum KE of H^- increases and the distribution becomes broader. However, the increase in the kinetic energy is not commensurate with increase in electron energy, indicating that the excess energy is shared between the translational energy and internal excitation of the NH_2 fragment.

Figure 2(b) shows the velocity image of the NH_2^- ions at 5.5 eV (see supplementary material[24] for NH_2^- velocity images at 4.5 and 6.5 eV). In spite of the small size of the image, it is discernible that the NH_2^- ions are ejected perpendicular to the electron beam similar to H^- ions. The maximum kinetic energy of the NH_2^- ions is found to be about 0.15 eV (see Figure 3(b)). The dissociation channel is understood to be $H(^2S) + NH_2^-(^1A_1)$ with appearance energy of 3.83 eV and correlates to an A_1 resonance state (see Table I) based on Wigner-Witmer correlation rules. Estimating the maximum kinetic energy of NH_2^- ions from this channel, it is about 0.1 eV which is 1/17th of the excess energy above threshold of 3.83 eV. The observed value of ~ 0.15 eV is close to the estimated value and confirms the presence of $H(^2S) + NH_2^-(^1A_1)$ channel and is consistent with the earlier findings.[6]

We analysed the angular distribution of H^- ions as a function of their kinetic energy (see Figure 4(a)). For H^- ions with maximum kinetic energy (i.e., above 1.2 eV), the an-

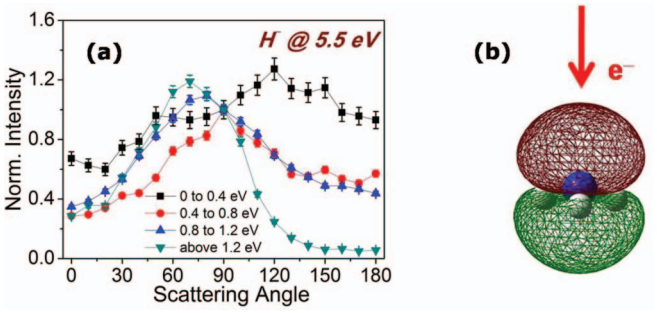

FIG. 4. (a) Variation of angular distribution of H^- ions as a function of the kinetic energy at 5.5 eV incident electron energy. The plots show angular distribution changing as function of KE or internal state of NH_2 fragment induced upon umbrella mode vibrations of the NH_3^{-*}. Similar behaviour is seen at other electron energies too (see supplementary material[24]). The angular distribution plots are normalized at 90°. (b) Schematic of the molecular geometry and $3a_1$ orbital orientation with respect to the incoming electron beam preferred for the DEA process at 5.5 eV.

gular distribution peaks close to 70° and falls off rapidly at forward and backward scattering angles with an asymmetry, i.e., forward angles (near 0°) are more intense than the backward (near 180°). However, for lower kinetic energies, especially below 0.8 eV, the angular distribution changes and the backward angles tend to get more intense. This variation in angular distribution with kinetic energy shows that the dissociation takes place with changing molecular geometry induced upon vibrational excitation. The excess energy is distributed as kinetic energy of the H^- ion and the internal energy of NH_2 fragment. Higher the kinetic energy of H^- ion, less is the internal excitation of the accompanying neutral fragment and possibly, less deviation from the equilibrium molecular geometry. From what we observe, the angular distribution of H^- ions peaks strongly about 70° at kinetic energies above 1.2 eV and becomes broad at lower kinetic energies (see Figure 4(a)). Infact, one can see two discernible maxima at angles close to 60° and 120° at lower kinetic energies (below 0.4 eV). Elaborating further, the ground state equilibrium geometry of NH_3 is pyramidal with N atom at the top and the three H atoms at the base of the pyramid. The three NH bonds are oriented at an angle 68.2° with respect to the C_3 axis passing through the N atom and the centre of the triangle formed by the three H atoms. The $3a_1$ orbital that is excited upon electron attachment has the electron density distributed above and below the plane perpendicular to this C_3 axis (see Figure 4(b)). It may be the case that upon electron attachment, the H^- ions that dissociate instantly carry away almost all the excess energy as translational kinetic energy and retain the orientation information of the dissociating N–H bond in the angular distribution. Therefore, for the most energetic ions the angular distribution peaks at 70° (close to 68.2°) and falls off at other angles in accordance with the ground state equilibrium geometry (C_{3v}). However, when the excess energy is used to induce umbrella mode vibrations, this reduces the KE of H^- and increases the angle between the N–H bonds and the C_3 axis from 70° and beyond 90°. When the dissociation occurs in this inverted geometry, H^- ions are scattered in the backward angles and are seen to be intense at lower kinetic energies of H^-. Thus, the electron attachment takes place preferentially in one orientation of ammonia molecule where the C_3 axis is along the electron beam direction (from N side to H side) and dissociation following umbrella mode vibrations gives rise to the observed variation in angular distribution. While it can be argued that the other orientation of the molecule with the N atom away contributes similarly, it cannot be reconciled to the fact that the angular distribution of the highest energy H^- ions peaks at 70° and not at 110° as should have been the case. This only indicates that the electron attachment probability is higher for one orientation and not for the other. The orbital picture shown in Figure 4(b) showing the lobes is merely suggestive of the geometry of the electron attachment process and does not represent the electron attachment probability.

We compared the angular distribution of H^- ions (KE ≥ 1.2 eV) at 5.5 eV electron energy with the measurement of Tronc *et al.*[9] – the only existing angular distribution measurement on ammonia (Figure 5(a)). Tronc *et al.*[9] reported the angular distribution of H^- ions for 5.7 eV incident electron energy and kinetic energy 1.3 eV in the angular range 20°–

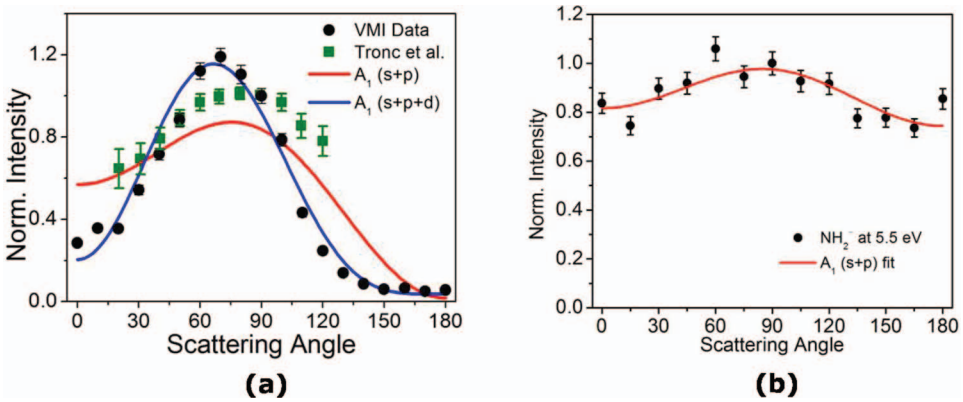

FIG. 5. (a) Angular distribution of H^- ions at 5.5 eV electron energy with maximum kinetic energy (above 1.2 eV) (black circles) obtained in our imaging experiment and comparison with the measurement of Tronc *et al.*[9] (green squares) at 5.7 eV incident electron energy and H^- ions of kinetic energy ~1.3 eV. The red and blue solid curves are fits obtained using A_1 symmetry functions taking $s + p$ and $s + p + d$ partial waves, respectively. (b)Angular distribution of NH_2^- ions at 5.5 eV electron energy. The red curve is the fit obtained using A_1 symmetry functions with s and p partial waves. The angular distribution plots are normalized at 90°.

120°. Comparison with our data shows a broad agreement with a peak about 80° and intensity falling off at lower and higher angles. However, the asymmetry about the peak in terms of intensities in the forward-backward angles cannot be compared as there are no data points close to those angles. Further, we fit our angular distribution data with A_1 symmetry functions to get a qualitative idea about the partial waves involved in the DEA process at 5.5 eV and find that *s*, *p*, and *d* waves contribute in the scattering of H^- ions. The fits are not tight enough in all cases and only give qualitative picture. (See supplementary material[24] on angular distribution fits). These fits are obtained for the molecule in C_{3v} geometry.

The angular distribution of NH_2^- ions arising from the $H + NH_2^-(^1A_1)$ channel (Figure 5(b)) looks more or less isotropic with a broad peak about 90°. However, as seen from the velocity slice image in Figure 2(b) (and in supplementary material[24]), it is discernible that the NH_2^- are scattered perpendicular to the electron beam. As understood from the H^- angular distribution from this resonance process peaking at 5.5 eV, the electron attachment to ammonia occurs preferentially along the C_3 axis (N side to H side). Similar to the H^- breaking away sideways with respect to the electron beam, it is possible that the H-NH_2 bond is dissociated with the extra electron retained on the NH_2 fragment and recoils opposite to the H atom. Thus, NH_2^- ions scattering perpendicular to the electron beam direction is on expected lines. However, being 16 times more massive than the H fragment, they carry very little kinetic energy and therefore, the radial size of the velocity slice image is small. This makes it difficult to resolve the angular distribution clearly and as a result the plot in Figure 5(b) look more or less flat (isotropic). Nevertheless, it is clear that NH_2^- ions are scattered perpendicular in this resonance process.

B. Second resonance process peaking at 10.5 eV

So far, there has been no report addressing the dissociation dynamics of the second resonance in ammonia. We report here, the kinetic energy and angular distribution details of the fragment anions from the DEA resonance process peaking at 10.5 eV for the first time. In an attempt to find the parent state of this resonance, we compare with VUV absorption and photoelectron spectra[20–22] reported in literature and find that the $1e \rightarrow 3sa_1$ Rydberg transition reported to occur at 85 000 cm^{-1} or 10.6 eV (Refs. 20, 21) is the parent state of the DEA resonance at 10.5 eV. The photoelectron spectra of ammonia[22] show two ionization processes corresponding to ionization of the $3a_1$ and 1e molecular orbitals at 10.15 eV and 14.92 eV, respectively. Rydberg transitions converging to these ionization potentials will occur at lower energies and therefore, the DEA resonance at 10.5 eV is due to the excitation of the HOMO-1 1*e* orbital. Excitation of such a doubly degenerate 1*e* orbital is expected to have a Jahn-Teller effect also.

Figure 6(a) shows the velocity slice image of H^- ions at 10.5 eV. We also obtained the images at other electron energies across the resonance (9.5 and 11.5 eV – see velocity images in supplementary material[24]). As seen from the velocity image, the scattering is strong in the backward direction. And Figure 6(b) shows NH_2^- ions scattered in forward direction. Similar forward scattering of NH_2^- is seen at 9.5 eV and 11.5 eV. The angular distributions of both the fragment ions are reminiscent of the angular distributions of ions produced from the dissociation of the $^2B_2$ resonance in water at 11.8 eV, where the H^- ions are scattered backward and the O^- ions are scattered in the forward direction.[23] The unique forward-backward scattering of the H^- and NH_2^- gives us information on the bond orientation at the instant of electron capture. It shows that the electron capture occurs with maximum probability when the electron is approaching along the H–N bond and that mostly this N–H bond is broken resulting in H^- ejected anti-parallel and NH_2^- ejected parallel to the direction of the electron.

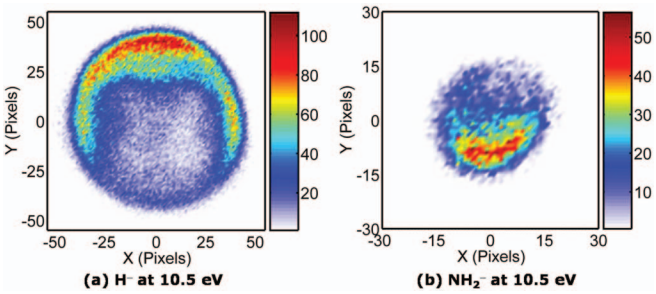

FIG. 6. Velocity slice images of H^- and NH_2^- ions from the second resonance process at 10.5 eV. The electron beam direction and the scattering angles are same as shown in Figure 2(a). The images show the impact coordinates of ions where every impact point corresponds to a particular velocity.

The kinetic energy of H^- ions ranges from 0 to about 5 eV (Figure 7(a)) at 10.5 eV electron energy and points to the dissociation channel $H^- + NH_2^*(^2A_1)$ (threshold: 5.23 eV). Had the products H^- and NH_2 been in their ground state (threshold: 3.85 eV), an excess energy of 6.65 eV would be shared amongst the two fragments. The maximum KE of H^- in such a case would be about 6.3 eV, which is higher than what we see. Whereas for $H^- + NH_2^*(^2A_1)$ channel, the maximum KE of H^- is estimated to be ~5.0 eV, which is what we observe. Hence, the dissociation channel is found to be $H^- + NH_2^*(^2A_1)$ where the neutral amino fragment is in the first electronic excited state.

In the case of NH_2^- ions, we find the maximum kinetic energy to be about 0.35 eV. (see Figure 7(b)). Amongst the possible dissociation channels, the $H + NH_2^-(^1A_1)$ channel with threshold of 3.83 eV would lead to NH_2^- fragment hav-

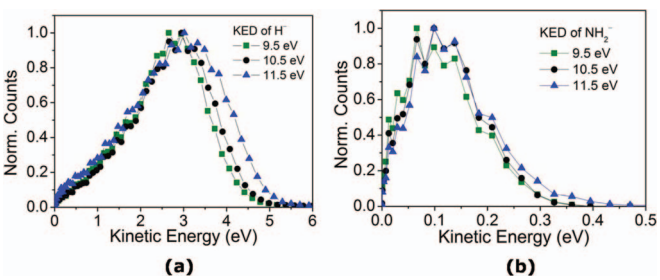

FIG. 7. Kinetic energy distribution of (a) H^- ions and (b) NH_2^- at 9.5, 10.5, and 11.5 eV across the second resonance.

ing maximum kinetic energy of 0.4 eV. This estimated value is close to what we observe, i.e., 0.35 eV. Further, as seen in Figure 7(b), the broad distribution could be attributed to the vibrational excitation of NH_2^-. Sharp and Dowell[6] speculated that the amino anion fragment produced at this resonance is in its first electronically excited state. A rough estimate suggests that presence of $H + NH_2^{-*}$ channel with appearance energy ~5 eV would produce those ions with energies close to 0.3 eV, close to what we find. However, there are no reports or data available on the electron affinity of NH_2^* that shed light on the stability/lifetime of the amino anion in the first excited state. In view of this, we cannot confirm the possibility of amino anion in the first excited state. The formation of vibrationally excited amino anion in ground electronic state explains the observed KE distribution.

Also, it is worth noting from the experiments of Compton *et al.*,[7] the existence of the NH^- fragment possibly arising from a three body breakup. Compton *et al.*[7] reported NH^- with a low yield, about a factor of 5 lower than NH_2^-. We cannot resolve NH^-/NH_2^- in our experiments. In the event of amide anion (NH^-) arising from a three body break up scheme $H + H + NH^-(^2\Pi)$ (threshold: 8.08 eV), Wigner-Witmer rules correlate such a three body channel with $NH^-(^2\Pi)$ state to E symmetry of the ammonia anion resonance. At an incidence electron energy of 10.5 eV, the excess energy available would be 2.42 eV and assuming this is distributed amongst the three fragments as translational kinetic energy, the maximum KE of NH^- would be 2/17th of 2.42 eV ~ 0.3 eV. When the two hydrogen atoms break away symmetrically, based on energy and momentum conservation, the kinetic energy of NH^- could be expressed as a function of the angle 2θ between the two dissociating bonds as, $E_{NH^-} = 2E_o \cos^2\theta/(15 + 2\cos^2\theta)$, where $E_o = 2.42$ eV. We observe that with θ varying from 0° to 90°, the KE of NH^- decreases from 0.3 to 0 eV. The peak value of 0.12 eV corresponds to $\theta = 53°$ (i.e., H-NH-H bond angle is 106°). Thus, symmetry and energy arguments allow for the three body channel giving rise to NH^- to exist.

So based on our data and the available literature, we conclude that the observed heavier anion is mostly NH_2^- in ground electronic state with internal excitation. While the presence of NH^- cannot be ruled out, its contribution would be lower by at least a factor of 5 as reported by Compton *et al.*[7] Since there would be a small flight time difference between the two ions and the velocity slice imaging is done at the center of the time-of-flight peak, the contribution from the NH^- (even if present) to the velocity slice image would be considerably smaller. It is highly desirable that potential energy surface calculations of NH_3^- resonance state and experiments with improved electron energy and mass resolution resolve this issue further.

Analyzing the angular distribution of H^- ions as a function of the kinetic energy release we see variation in the angular distributions indicating structural changes of the ammonia anion. Figure 8(a) shows angular plots of H^- ions as function of kinetic energy. It is seen that the ions with maximum KE (i.e., above 4 eV) show an angular distribution with peaks at 60° and 180°. As the kinetic energy decreases, the backward angles become more intense. We explain the observed angular distribution and its variation with the kinetic energy of the ion in terms of the electron attachment to the doubly degenerate 1*e* orbital (see Figure 8(b)). The electron density in the 1*e* orbital is distributed encompassing the NH bonds. If the electron capture occurs when one of the H-N bond is oriented along the electron beam, instant dissociation of the ammonia anion may lead to breaking any of the three N–H bonds. The ions with largest kinetic energy correspond to the instantaneous fragmentation before the excess energy can be redistributed into other vibrational modes. While one N–H bond is antiparallel to the electron beam, the other two are oriented at approximately 60° with respect to the electron beam. Thus, we see peaks at 60° and 180° in the angular distribution of H^- ions with highest kinetic energy (Figure 8(a)). The excess energy in the system can go into the excitation of the vibrational modes and the bending mode may reduce the H–N–H bond angle from 120° to 90° while causing the H-N bond along the electron beam to stretch and eventually eject the H^-. The probability of H^- ejected from the other two N–H bonds (oriented close to 90° with respect to the electron due to bending mode vibrations) seems to be lower than at 180° direction, giving rise to the backward distribution. We fit the angular distribution of H^- ions with highest kinetic energy with functions of E symmetry taking the lowest allowed *p* and *d* partial waves. The

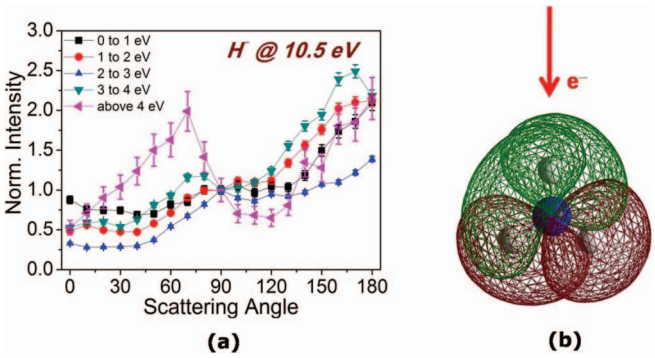

FIG. 8. (a) Angular distribution of H^- ions as a function of kinetic energy at incident electron energy of 10.5 eV. The variation in angular distribution shows rearrangement of the molecular geometry prior to dissociation due to vibrational motion suggesting deviation from axial recoil approximation. The angular distribution plots are normalized at 90°. (b) Schematic of the doubly degenerate HOMO-1 1*e* orbital (superposed) and the molecular orientation preferred for the second resonance process at 10.5 eV.

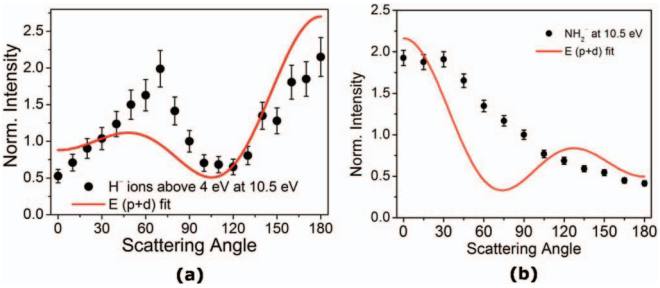

FIG. 9. Angular distribution of H^- and NH_2^- ions at electron energy of 10.5 eV. The red curve is the fit for two body breakup using *E* symmetry functions taking *p* and *d* partial waves. The angular distribution plots are normalized at 90°.

fit in Figure 9(a) reproduces the forward backward asymmetry qualitatively but is far from a good fit. Considering the double degeneracy of the 1*e* orbital, this could be a manifestation of Jahn-Teller effects or other non-adiabatic effects leading to rapid distortion of the molecular geometry.

While the H-N bond oriented along the electron beam dissociates to give H^- ions in the backward direction, the NH_2 fragments must recoil in the forward direction in line with momentum conservation. When the extra electron is taken by the NH_2 fragment instead of the H, we see the forward scattered NH_2^- like in Figure 6(b). Figure 9(b) shows the angular distribution of NH_2^- fragment at 10.5 along with the fit of *E* symmetry. Again, we see that the fit qualitatively reproduces the finite intensities at the forward backward angles along with the asymmetry, but is not a very good fit. The lack of a good fit indicates that the dissociation into $H + NH_2^-$ does not follow axial recoil approximation.

IV. CONCLUSIONS

We report here first ever measurements of the kinetic energy and angular distribution of the H^- and NH_2^- fragment anions across the two negative ion resonances in ammonia peaking at 5.5 eV and 10.5 eV, respectively, based on the velocity slice imaging technique. The first resonance peaking at 5.5 eV has $A_2^{''}(D_{3h})$ (or A_1 (C_{3v})) symmetry and dissociates into $H^- + NH_2(^2B_1)$ and $H + NH_2^-(^1A_1)$ channels. Variation in the angular distribution of the H^- ions with kinetic energy is attributed to umbrella mode vibrations ν_2 of the ammonia anion. The second resonance peaking at 10.5 eV shows strong anisotropy in the angular distributions of the ions with H^- scattered in the backward hemisphere and NH_2^- in the forward hemisphere. The H^- ions are produced through the $H^- + NH_2^*$ (threshold: 5.23 eV) channel where the amino fragment is in the first excited state. The amino anion fragment is inferred to come from $H + NH_2^-$ channel where NH_2^- is in electronic ground state but vibrationally excited. Based on the analysis of the H^- ions with highest kinetic energy, the resonance is found to have *E* symmetry within the C_{3v} geometry.

[1] J. M. Greenberg, Surf. Sci. **500**, 793 (2002).
[2] M. P. Bernstein, J. P. Dworkin, S. A. Sandford, G. W. Cooper, and L. J. Alamandola, Nature (London) **416**, 401 (2002).
[3] P. D. Holtom, C. J. Bennet, Y. Osamura, N. J. Mason, and R. I. Kaiser, Astrophys. J. **626**, 940 (2005).
[4] V. S. Prabhudesai, A. H. Kelkar, D. Nandi, and E. Krishnakumar, Phys. Rev. Lett. **95**, 143202 (2005).
[5] S. Ptasinska, S. Denifl, V. Grill, T. D. Mrk, P. Scheier, S. Gohlke, M. A. Huels, and E. Illenberger, Angew. Chem., Int. Ed. **44**, 1647 (2005).
[6] T. E. Sharp and J. T. Dowell, J. Chem. Phys. **50**, 7 (1969).
[7] R. N. Compton, J. A. Stockdale and P. W. Reinhardt, Phys. Rev. **180**, 111 (1969).
[8] K. L. Stricklett and P. D. Burrow, J. Phys. B **19**, 4241 (1986).
[9] M. Tronc, R. Azria, and M. B. Arfa, J. Phys. B **21**, 2497 (1988).
[10] P. Rawat, V. S. Prabhudesai, M. A. Rahman, N. Bhargava Ram, and E. Krishnakumar, Int. J. Mass Spectrom. **277**, 96 (2008).
[11] A. E. Douglas, Discuss. Faraday Soc. **35**, 158 (1963).
[12] D. H. Mordaunt, M. N. R. Ashfold, and R. N. Dixon, J. Chem. Phys. **104**, 6460 (1996).
[13] K. R. Lykke, K. K. Murray, and W. C. Lineberger, Phys. Rev. A **43**, 6104 (1991).
[14] J. Xin, H. Fan, I. Ionescu, C. Annesley, and S. A. Reid, J. Mol. Spectrosc. **219**, 37 (2003).
[15] C. T. Wickham-Jones, K. M. Ervin, G. B. Ellison, and W. C. Lineberger, J. Chem. Phys. **91**, 2762 (1989).
[16] R. P. Saxon, B. H. Lengsfield, and B. Liu, J. Chem. Phys. **78**, 312 (1983).
[17] D. M. Neumark, K. R. Lykke, T. Anderson, and W. C. Lineberger, J. Chem. Phys. **83**, 4364 (1985).
[18] D. Nandi, V. S. Prabhudesai, E. Krishnakumar, and A. Chatterjee, Rev. Sci. Instrum. **76**, 053107 (2005).
[19] P. Chantry, J. Chem. Phys. **55**, 2746 (1971).
[20] A. D. Walsh and P. A. Warsop, Trans. Faraday Soc. **57**, 345 (1961).
[21] M. B. Robbins, *Higher Excited States of Polyatomic Molecules* (Academic, 1974), Vol 1.
[22] G. R. Branton, D. C. Frost, F. G. Herring, C. A. McDowell, and I. A. Stenhouse, Chem. Phys. Lett. **3**, 581 (1969).
[23] N. Bhargava Ram, V. S. Prabhudesai, and E. Krishnakumar, J. Phys. B **42**, 225203 (2009).
[24] See supplementary material at http://dx.doi.org/10.1063/1.4705358 for velocity slice images and angular distributions across the two resonances and details of the C_{3v} angular functions and fit parameters.